

# High energy power-law tail in X-ray binaries spectrum and bulk Comptonization due to a conical outflow from a disk

Nagendra Kumar\*

Department of Physics, Indian Institute of Science, Bangalore 560012, India

(Dated: December 14, 2024)

The observed high energy power-law tail of high soft (HS) state, and steep power law (SPL) state of X-ray binaries can be generated by the bulk Comptonization process with a free-fall bulk region onto the compact object. We study these high energy tails by considering a bulk region arisen due to a right circular conical outflow (of opening angle  $\theta_b$  with axis perpendicular to the disk) from the disk, using a Monte Carlo scheme. Out of two possible bulk directions, i) along the surface of the cone, ii) inside the conic region, we find that a) the randomness of bulk directions is increased with increasing  $\theta_b$ , b) the emergent spectrum has a power-law component in the observed range of photon index  $\Gamma$  ( $> 2.4$ ) in both cases for  $\theta_b$  greater than  $\sim 30$  degree, even for a low medium temperature. For given  $\Gamma$ , the optical depth for lower opening angle has comparatively high value than the case with larger opening angle of conical outflow. Similarly the bulk speed is higher for smaller opening angle. It seems that the lower opening angle outflow can provide the observed high energy tail in both the states HS and SPL. We notice that when the outflow is collimated or conical flow ( $\theta_b < 30$ ) then the emergent spectrum does not have power-law component unless it is observed in thermal Comptonized spectrum.

PACS numbers: 95.30.Gv, 95.30.Jx, 95.85.Nv, 97.10.Gz, 97.80.Jp, 97.60.Lf

*Introduction* – Black hole (BH) X-ray binaries (XRBs) frequently change their X-ray spectral states particularly power-law dominated low intense hard (LH) state to blackbody dominated high intense soft (HS) state via outburst which again settles down to the LH state. The outburst generally occurs on the time scale of months to years, and the recurrence time scale varies even for the same source. During the spectral state transition, some times a very high intense power-law dominated (VHS) state is observed where the photon index  $\Gamma$  is greater than 2.4, which is also termed as a steep power law (SPL) state, and the spectrum generally extends upto more than 200 keV without an exponential cut-off. In the hardness intensity diagram (or Q-diagram), the VHS state is observed in upper-right region, where occasionally an episodic jet is observed (for review, see, 1–5; in particular, 6–10). In HS state also, often a high energy power-law tail is observed which may be extended up to 200 keV or more with photon index greater than 2.0 [see, e.g., 11–13]. The high energy tail in the soft state is also observed in neutron star (NS) low mass X-ray binaries (LMXBs) [e.g., 14, 15]. The physical origins of the SPL state and observed high energy power-law tail during HS state are unclear, however there are so many models available in literature which deal either in terms of underlying radiative process or in a more rigorous way by studying the accretion flows [e.g., 16].

In the thermal Comptonization process, where soft photons are upscattered by high energetic electrons, the high energy power-law tail can be produced with electron medium temperature 100 keV and optical depth around unity [15, 17]. Mainly, three models are proposed to explain the power-law tail in the frame work of modified Comptonization. The first one is non-thermal Comp-

tonization where a disk (as a source of soft photon) and Comptonizing medium (corona, or a sub-Keplerian advective part, e.g., 18) are energetically coupled to each other, unlike the case of thermal Comptonization where both are decoupled. This model has been primarily developed by Done and Kubota [19], which is further revised by Kubota and Done [20]. Second one is a hybrid model, in which a hybrid electron distribution is considered, where electron velocity distribution consists of both the thermal (Maxwellian) distribution and non-thermal (power-law) distribution parts [21, 22]. The last one is the bulk Comptonization where photons are upscattered due to both thermal and bulk motions of the electrons. The bulk Comptonization model for SPL state was primarily developed by Titarchuk *et al.* [23], where the bulk motion is due to a free-fall converging flow of spherically accreted plasma into BH and the seed photons are supplied from the outside of the free-fall region. Later, the bulk Comptonization model was developed for NS sources with the same inflow geometry [e.g., 24–26].

In this letter, we explore another possibility for power-law component of SPL and high-energy power-law tail of HS state in a frame work of the bulk Comptonization with the consideration of an outflow geometry. To compute the emergent spectrum, we use a Monte Carlo Scheme. We find that when the outflow is a conical type, then the soft photons can get upscattered and the emergent spectra have a power-law component. Although, Laurent and Titarchuk [27] have developed a Monte Carlo code with spherically divergent type of outflow, they noticed only downscattering of the soft spectrum [see also, 28, 29].

*Monte Carlo Method* – The bulk Comptonization process was initially formulated by Blandford and Payne

[30, 31]. Later, Titarchuk *et al.* [23] studied the bulk Comptonization for a converging inflow material (which was a prediction of Chakrabarti and Titarchuk [32], when they tried to understand the HS state) to explain the power-law component seen in BHXRBs. In this work, we develop a Monte Carlo (MC) code for a bulk Comptonization by considering an outflow geometry (Comptonizing) and we do not take an account of the effects of general relativity. The algorithm for MC code is similar to that of Kumar and Misra [33] for a thermal Comptonization part and for the bulk motion effect we adopt a similar to that discussed by Laurent and Titarchuk [34], Niedźwiecki and Zdziarski [35] by neglecting general relativistic effects. Due to a bulk motion of the medium, the mean free path of the photons will increase compared to that of the static medium. The mean photon free path is calculated following Sazonov and Sunyaev [36] and in our calculation we consider the composite speed of thermal and bulk speed for a final electron speed. The average energy exchange per scattering for a monochromatic photon of energy  $E$  in corona having temperature  $kT_e$  and a bulk flow with constant speed  $u_b$  Titarchuk *et al.* [23] is  $\Delta E = \Delta E_{TH} + \left( \frac{4u_b}{c\tau} + \frac{(u_b/c)^2}{3} \right) \frac{E}{m_e c^2}$ . Here,  $\Delta E_{TH} = (4kT_e - E) \frac{E}{m_e c^2}$  is for thermal Comptonization i.e.,  $u_b = 0$ ,  $\tau$  is the optical depth of the scattering medium,  $c$  is the speed of light,  $m_e$  is the rest mass of the electron and  $k$  is Boltzmann constant.

For the given two sets of  $kT_e$  and  $u_b$ , it is possible that  $\Delta E$  would be same, and so the single scattering spectrum would be identical for both sets. This is also valid for multiple scattering spectrum if the average scattering number  $\langle N_{sc} \rangle$  be same. We use this fact to check the MC code by comparing the simulated bulk Comptonized spectrum to thermal Comptonized (i.e.,  $u_b = 0$ ) one. For example, for the two sets ( $kT_e = 3$  keV,  $u_b = 0$ ) and ( $kT_e = 2$  keV,  $u_b = 0.0766$  c) the energy exchange per scattering  $\Delta E$  is same, however in this calculation we neglect the contribution of term  $\frac{4u_b}{c\tau}$ . We compute the emergent spectrum for both sets by considering a random bulk motion. We find, the spectrum is identical for both sets, either in single scattering or multiple scattering, which are shown in Fig. 1 by curve 1 and 2 respectively. The results have been also checked by the Wien peak spectrum, i.e. when the corresponding  $\langle N_{sc} \rangle$  is very large ( $\sim 500$ ), shown as curve 3 in Fig. 1 with above two sets of parameters. We also check the MC results in a bulk motion dominated regime (i.e.,  $(u_b/c)^2 \gg 3kT_e/(m_e c^2)$ ) by analysing the Wien peak. We compare our Monte Carlo results with the existing results of Laurent and Titarchuk [34] for spherical inflow type of bulk motion, where they argued that for flat geometry (i.e. without general relativity), the photon index of power-law tail is always less than  $\sim 2.1$ , even if lower value of  $\dot{m}$  (a ratio of mass accretion rate to the Eddington rate) = 1, which correspond to  $\tau = 0.7$  (see their Table 1). We

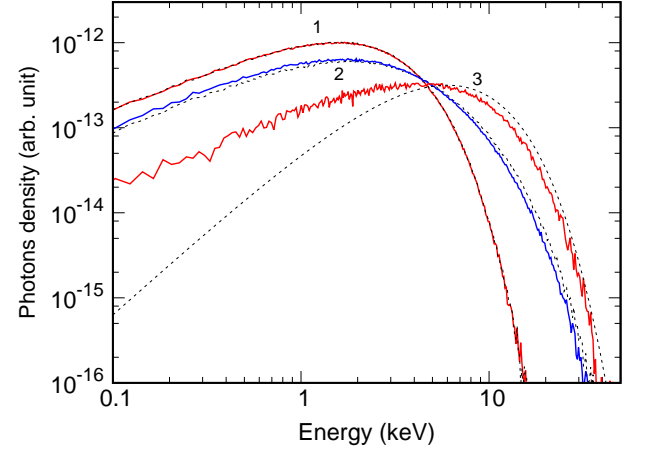


FIG. 1. Spectra comparing Monte Carlo results (for bulk Comptonization) with analytical ones, i.e., thermal Comptonization. The curves 1, 2, and 3 are for single scattering, multiple scattering ( $\langle N_{sc} \rangle \sim 46$ ), and Wien peak ( $\langle N_{sc} \rangle > 500$ ). The solid lines are for bulk Comptonization and dashed lines are for thermal Comptonization. The free parameters for bulk Comptonization are  $kT_e = 2$  keV,  $\tau = 12.5$ ,  $u_b = 0.0766$  c and for thermal Comptonization are  $kT_e = 3$  keV,  $\tau = 9$ ,  $u_b = 0.0$ . In all cases, the seed photon source temperature  $kT_b = 1.0$  keV.

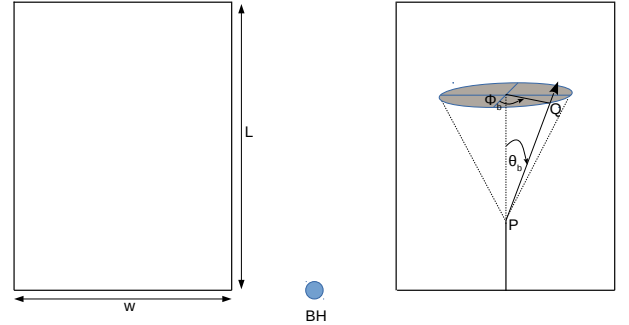


FIG. 2. Meridional cut of a rectangular torus surrounding the BH. The conical shaded region at a scattering point P is a possible direction of the bulk motion. Here PQ is one bulk direction which has  $\theta_b$  &  $\phi_b$  angle in global coordinate,  $w$  is width of the torus and  $L$  is the height of the torus but both are not in scale.

find that our results are consistent.

*Emergent spectrum from Outflow geometry* – We assume that the outflow occurs on the disk, and for an outflow region, we consider a torus surrounding the compact object, which has a rectangular cross-section [e.g., 33]. We assume that the torus is located far away from the compact object, so that the general relativistic effect is unimportant. The meridional cut of the torus is shown in Fig. 2. We fix a global spherical polar coordinate  $(r, \theta,$

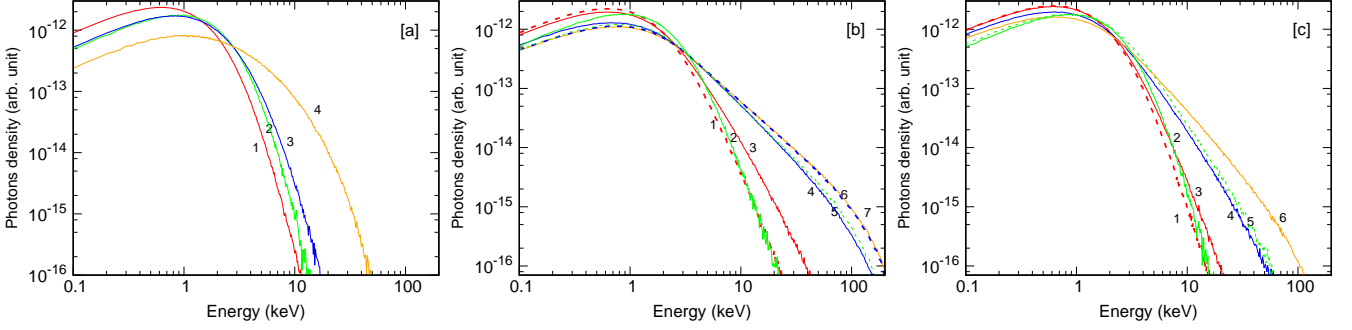


FIG. 3. The simulated emergent spectra for different outflow geometry as functions of outflow direction. The left is for collimated outflow, while middle and right panels are for case I and II in conical outflow respectively. In left panel the curves 1,2,3 and 4 are for  $\theta_b = 0$  (outflow), 180 (inflow), 90 and 90 degree. In middle and right panel the curves 1,2,3,4,5, and 6 are for  $\theta_b = 20, 160, 30, 60, 110,$  and 90 degree respectively. In middle panel the curve 7 (dashed) is for 95 degree. The spectral parameters for all curves are  $kT_e = 3.0$  keV,  $kT_b = 0.5$  keV,  $\tau = 3$  and  $u_b = 0.45$  c except for 4th curve of left panel where  $\tau = 15$  and  $u_b = 0.65$  c

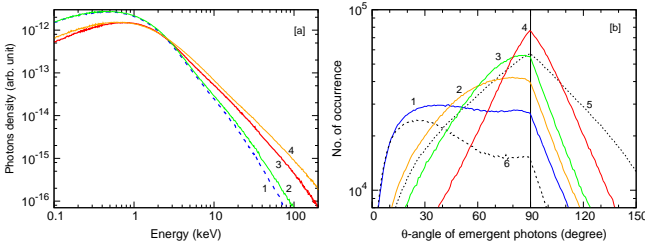


FIG. 4. The left panel is for an emergent spectra and right panel is for  $\theta$ -angle distribution of the emergent photons. In left panel, the curves 1 is for collimated flow with  $\theta_b = 15$  degree, and the curves 2, 4 are for conical flow with  $\theta_b = 15,$  and 45 degree respectively, with  $u_b = 0.75$  c and  $kT_e = 30.0$  keV (i.e., bulk dominated case  $(u_b/c)^2 \gg 3kT_e/(m_e c^2)$ ). The curve 3 is for a thermal dominated case. In right panel, the curves 1, 2, 3, 4 are for conical flow with  $\theta_b$  15, 45, 60, 90 degree and bulk speed 0.75 c, and the curve 6 is for  $\theta_b = 15$  degree and  $u_b = 0.85$  c. The curve 5 is for thermal dominated case. The rest parameters are  $kT_b = 0.5$  keV,  $kT_e = 30.0$  keV and  $\tau = 1$ .

$\phi$ ) at the center of the torus. Without any loss of generality, we assume, the torus exists only above the equatorial plane, and when the scattered photons cross the equatorial plane, these photons will get absorbed. The width of the torus  $w$  is fixed to 10 km and a vertical height  $L$  to 1 km. We assume that the optical depth is along the vertical direction so that the electron density in the torus is  $n_e = \frac{\tau}{L\sigma_T}$ . We assume that the seed photon source is inside the torus and it is a blackbody at temperature  $kT_b$  which emits vertically from the equatorial plane.

For the outflow geometry, we consider a right circular conical outflow of opening angle  $\theta_b$ , with the axis perpendicular to the equatorial plane (i.e., along the positive  $z$ -axis), which originates from each point inside the torus on the equatorial plane. The possible outflow direction at any point inside the torus can be any direction inside

the conical region from the vertex of that cone, as shown by the shaded region in Fig. 2, and we assigned the bulk direction locally by the same global coordinate with  $(\theta_b, \phi_b)$ , as shown in Fig. 2. We are first interested to study a collimated bulk flow. With the definition of a conical outflow, the collimated flow is determined from  $\theta_b = \text{constant}$ , and  $\phi_b \equiv \phi$ -angle of vertex of cone in global coordinate. We select the flow direction which is away from the compact object. For example,  $\theta_b = 0$  and 180 degree are vertically upward and vertically downward collimated outflow respectively.

The emergent spectra for collimated outflow are shown in Fig. 3a. We do not find a high energy power-law tail in the collimated flow even in the extreme condition like curve 4 of Fig. 3a. Our results are consistent with Janiuk *et al.* [37] that the multiple scattering spectra in inflow is red-shifted from single scattering spectra. However, if the medium temperature is sufficient high, the high energy power-law tail can be generated by thermal Comptonization process, i.e., without any bulk flow [e.g., 15, 29]. We find that when  $kT_e$  greater than  $\sim 25$  keV, the power-law tail can be extended upto 200 keV, which is shown by the curve 3 in Fig. 4a and here the curve 1 is for a collimated flow with  $\theta_b = 15$  degree. Hence, for a collimated outflow/inflow, If the high energy power-law tail can not be generated through a thermal Comptonization process then it also not found in the bulk Comptonized spectra.

Next we consider two different plausible cases of conical bulk outflow geometry. In case I, we simply consider, the bulk motion direction is in any one direction on the surface of the cone from the vertex as shown in Fig. 2. That is, the  $\theta_b$  is fixed to a constant value and  $\phi_b$  varies from 0 to  $2\pi$  in this case. In case II, the bulk direction can be any one directions from the vertex within the conical region as shown in Fig. 2. Therefore, in this case  $\theta_b$  will vary from 0 to  $\theta_b$ , and like case I  $\phi$  will vary from 0 to  $2\pi$ . The computed spectrum for both types of

TABLE I. The extreme sets of bulk speed  $u_b$  and optical depth  $\tau$  when the photon index  $\Gamma$  (for a power-law tail) is  $\sim 2.5$  at a given opening angle  $\theta_b$  of conical outflow (case I). The rest of the parameters are  $kT_b = 0.5$  keV,  $kT_e = 3.0$  keV

A set of $(u_b, \tau)^a$ at given $\theta_b$			
$\theta_b=30^\circ$	$\theta_b=45^\circ$	$\theta_b=60^\circ$	$\theta_b=90^\circ$
(0.8c, 5.25) ; (0.72c, 2.0) ; (0.6c, 1.9) ; (0.6c, 1.)			
(0.85c, 4.2)	(0.85c, 1.2)	(0.7c, 1.2)	

<sup>a</sup> this set value will also depend on  $kT_e$ , in this calculation  $\Gamma = 2.5$  is valid at least in  $\sim 40 - 200$  keV range.

conical outflows, case I and II have been shown in Fig. 3b and 3c respectively. We compute these spectra for 6 different opening angles  $\theta_b = 20, 160, 30, 60, 110$ , and  $90$  degree, which are shown in the curves 1, 2, 3, 4, 5, and 6 respectively. We noticed, the spectrum would be similar for both conical outflow, or inflow at given opening angle  $\theta_b$  (e.g., curve 1 and 2 in Fig. 3b and c).

For case I (i.e., Fig. 3b), the photon index of high energy tail varies from  $\sim 4$  to  $\sim 1.7$ , while for case II (i.e., Fig. 3c) the photon index varies from  $\sim 4.5$  to  $\sim 2.2$ , by varying  $\theta_b$  from  $20$  to  $90$  degree. Since the photon index decreases with increasing opening angle (from  $0$  to  $90^\circ$ ) of conical bulk flow (while the rest spectral parameters are same), the corresponding high energy cutoff will also increase. For example, in case II, the high energy cutoff for the spectrum is  $20$  keV and  $110$  keV when  $\theta_b = 20^\circ$  and  $90^\circ$  respectively. In Table I for a conical flow of case I, we summarise the extreme sets of  $u_b$  and  $\tau$  for a given parameters sets when the photon index is  $\sim 2.5$  (a typical  $\Gamma$  for high energy power-law tails), which extends at least up to  $\sim 200$  keV. We unable to find the observed  $\Gamma$  range in high energies power-law tails for  $\theta_b$  less than  $\sim 30$  degree. Hence, the bulk Comptonization process in a bulk conical outflow (with  $\theta_b > 30$  degree), which is originated at the accretion disk, is a plausible process for generating the high energy power-law tail in both states SPL and HS.

Expectantly, the photon index decreases with  $\tau$ . However,  $\Gamma$  decreases with  $u_b$  for  $\theta_b > 30$  degree, while it increases for  $\theta_b$  less than  $30$  degree in conical flow. In collimated flow, for all  $\theta_b$ ,  $\Gamma$  increases with  $u_b$ . This is shown in Fig. 4a. In Fig. 4b, the distribution of  $\theta$ -angle of emergent photons is shown for a conical flow (case I) with four different bulk direction  $\theta_b = 15, 45, 60$  and  $90$  degree. It seems that the emergent photons are in the direction of a bulk motion and it tends to be more along a bulk direction with a large value of  $u_b$ . These are also valid for a collimated flow. By the comparison of  $\theta_b$  distribution of emergent photons from thermal dominated one, we emphasized that in a conical flow the randomness of the bulk direction is increased with increasing  $\theta_b$  and for  $\theta_b = 90$  degree, it is a completely random. In collimated flow, since the  $\phi$ -angle is fixed, so it has very

less randomness in comparison to the conical flow and correspondingly the emergent spectra is softer, which is shown by the curves 2 and 3 in Fig. 4a. As the collimated case, in a conical flow for  $\theta_b$  less than  $30$  degree, the power-law tails can be produced when the power-law tails are also produced in thermal dominated regime.

*Summary and Discussion* — Using a Monte Carlo scheme, we simulate the emergent spectrum by bulk Comptonization process with the consideration of right circular conic outflow from the disk. The axis of cone is assumed to be perpendicular to the equatorial plane. We consider the outflow region lies inside a torus region. The soft photon is generated inside the torus region on equatorial plane, which is emitted vertically. However, in this paper we are not worrying about the physical origin of such a conical bulk flow, but our motivation is just to generate the observed high energy power-law tail during a high soft state, and a very high soft state of the X-ray binaries through bulk Comptonization process. Although, Titarchuk *et al.* [29] have modeled the gamma-ray burst spectrum, especially its high-energy power-law components, by the bulk Comptonization of the soft photon (emitted by star) by subrelativistic outflow, they considered a thermal motion dominated regime with taking the medium temperature  $kT_e \sim 100$  keV.

We first compute the emergent bulk Comptonized spectrum for the collimated outflow from the accretion disk or collimated inflow towards the disk. Next we consider a right circular conical outflow/inflow bulk motion, we look two different situations of bulk direction, in case I, the bulk direction is in any one direction along the surface of the cone, and in case II, the bulk direction is in any one direction within the conical region from the vertex. Like a collimated flow case, we observe that the spectrum is similar for both conical outflow and inflow with having same opening angle. We find, the emergent spectrum of case I is more harder than the case II. The photon index of power-law component in emergent spectrum for both cases decreases with increasing opening angle of cone  $\theta_b$ . However, we do not compare the emergent spectrum with observed spectrum, which we intended to do in a future work. Moreover, in Table I, we summarize the bulk Comptonization parameters for  $\Gamma = 2.5$  in conical flow. We find that the observed photon index can be accomplished only when the opening angle of conical bulk outflow  $\theta_b$  is greater than  $\sim 30$  degree. For  $\theta_b < 30$  degree and for collimated flow, the high-energies power-law tail would be also generated, when it is also found in thermal dominated case.

In conical flow, the randomness of bulk direction is increased with increasing  $\theta_b$ , and it is a complete random for  $\theta_b = 90$  degree. We find that for given  $\Gamma$ , the lower opening angle conical outflow/inflow has larger optical depth at given bulk speed, and it has larger  $u_b$  at given  $\tau$  in comparison to the higher opening angle conical flow. It seems that the lower opening angle conical

outflow/inflow may be responsible for high energy power-tail in both states, high soft state, and the steep power law state. Observationally, a spectral state dependent wind outflow (with speed less than 0.5 c) has been seen in low mass X-ray binaries [eg. 38, 39]. However, a correlation study between high energy power-law tail and wind (even jet) outflow may serve a physical origin of bulk Comptonization due to an outflow from the disk.

The high energy power-law tail can be produced within the bulk Comptonization framework either due to a conical type bulk flow, or due to a spherically free-fall type of bulk flow. For a free-fall bulk region, there is a physical motivation [32], and those models are explaining the observed power-law tail in a general relativistic regime [e.g., 27, 40]. However, Zdziarski *et al.* [41] argued that a bulk Comptonization due to a free-fall region can not explain the observed energy cutoff which is usually extended larger than 200 keV [see also, 14]. In conical type of bulk Comptonization, it is possible that the high energy cut-off can extend more than 200 keV, even for low medium temperature, depending upon bulk speed and optical depth (e.g., upper extreme case in Table I). But one has to find the physical mechanism for such a conical bulk flow from the accretion disk which will constrain its physical parameters like  $u_b$ , optical depth, angular distribution. It is also needed to consider a general relativistic effects in this calculation.

## ACKNOWLEDGEMENTS

NK acknowledges financial support from Indian Space Research Organisation (ISRO) with research Grant No. ISTC/PPH/BMP/0362. NK wishes to thank Ranjeev Misra for valuable comments on this project and Bani-brata Mukhopadhyay for their valuable suggestions and comments over the manuscript.

---

\* nagendra.bhu@gmail.com

- [1] J. E. McClintock and R. A. Remillard, “Black hole binaries,” in *Compact stellar X-ray sources*, edited by W. H. G. Lewin and M. van der Klis (2006) pp. 157–213.
- [2] C. Done, M. Gierliński, and A. Kubota, *A&A Rev.* **15**, 1 (2007).
- [3] T. M. Belloni, S. E. Motta, and T. Muñoz-Darias, *Bulletin of the Astronomical Society of India* **39**, 409 (2011).
- [4] R. Fender and T. Belloni, *Science* **337**, 540 (2012).
- [5] B. E. Tetarenko, G. R. Sivakoff, C. O. Heinke, and J. C. Gladstone, *ApJS* **222**, 15 (2016).
- [6] D. Debnath, S. K. Chakrabarti, A. Nandi, and S. Mandal, *Bulletin of the Astronomical Society of India* **36**, 151 (2008).
- [7] R. J. H. Dunn, R. P. Fender, E. G. Körding, T. Belloni, and C. Cabanac, *MNRAS* **403**, 61 (2010).
- [8] A. Nandi, D. Debnath, S. Mandal, and S. K. Chakrabarti, *A&A* **542**, A56 (2012).
- [9] J. E. McClintock, R. A. Remillard, M. P. Rupen, M. A. P. Torres, D. Steeghs, A. M. Levine, and J. A. Orosz, *ApJ* **698**, 1398 (2009).
- [10] M. Pahari, J. S. Yadav, and S. Bhattacharyya, *ApJ* **783**, 141 (2014).
- [11] A. Joinet, E. Jourdain, J. Malzac, J. P. Roques, V. Schönfelder, P. Ubertini, and F. Capitanio, *ApJ* **629**, 1008 (2005).
- [12] S. Motta, T. Belloni, and J. Homan, *MNRAS* **400**, 1603 (2009).
- [13] L. Titarchuk and N. Shaposhnikov, *ApJ* **724**, 1147 (2010).
- [14] M. G. Revnivtsev, S. S. Tsygankov, E. M. Churazov, and R. A. Krivonos, *MNRAS* **445**, 1205 (2014).
- [15] L. Titarchuk, E. Seifina, and C. Shrader, *ApJ* **789**, 98 (2014).
- [16] J. D. Schnittman, J. H. Krolik, and S. C. Noble, *ApJ* **769**, 156 (2013).
- [17] M. L. Parker, J. A. Tomsick, J. A. Kennea, J. M. Miller, F. A. Harrison, D. Barret, S. E. Boggs, F. E. Christensen, W. W. Craig, A. C. Fabian, F. Fürst, V. Grinberg, C. J. Hailey, P. Romano, D. Stern, D. J. Walton, and W. W. Zhang, *ApJ* **821**, L6 (2016).
- [18] S. R. Rajesh and B. Mukhopadhyay, *MNRAS* **402**, 961 (2010).
- [19] C. Done and A. Kubota, *MNRAS* **371**, 1216 (2006).
- [20] A. Kubota and C. Done, *MNRAS* **458**, 4238 (2016).
- [21] P. S. Coppi, in *High Energy Processes in Accreting Black Holes*, *Astronomical Society of the Pacific Conference Series*, Vol. 161, edited by J. Poutanen and R. Svensson (1999) p. 375.
- [22] M. Gierliński, A. A. Zdziarski, J. Poutanen, P. S. Coppi, K. Ebisawa, and W. N. Johnson, *MNRAS* **309**, 496 (1999).
- [23] L. Titarchuk, A. Mastichiadis, and N. D. Kylafis, *ApJ* **487**, 834 (1997).
- [24] A. Paizis, R. Farinelli, L. Titarchuk, T. J.-L. Courvoisier, A. Bazzano, V. Beckmann, F. Frontera, P. Goldoni, E. Kuulkers, S. Mereghetti, J. Rodriguez, and O. Vilhu, *A&A* **459**, 187 (2006).
- [25] R. Farinelli, A. Paizis, R. Landi, and L. Titarchuk, *A&A* **498**, 509 (2009).
- [26] R. Farinelli, L. Titarchuk, A. Paizis, and F. Frontera, *ApJ* **680**, 602-614 (2008).
- [27] P. Laurent and L. Titarchuk, *ApJ* **656**, 1056 (2007).
- [28] D. Psaltis, *ApJ* **555**, 786 (2001).
- [29] L. Titarchuk, R. Farinelli, F. Frontera, and L. Amati, *ApJ* **752**, 116 (2012).
- [30] R. D. Blandford and D. G. Payne, *MNRAS* **194**, 1033 (1981).
- [31] R. D. Blandford and D. G. Payne, *MNRAS* **194**, 1041 (1981).
- [32] S. Chakrabarti and L. G. Titarchuk, *ApJ* **455**, 623 (1995).
- [33] N. Kumar and R. Misra, *MNRAS* **461**, 4146 (2016).
- [34] P. Laurent and L. Titarchuk, *ApJ* **511**, 289 (1999).
- [35] A. Niedźwiecki and A. A. Zdziarski, *MNRAS* **365**, 606 (2006).
- [36] S. Y. Sazonov and R. A. Sunyaev, *A&A* **354**, L53 (2000).
- [37] A. Janiuk, B. Czerny, and P. T. Życki, *MNRAS* **318**, 180 (2000).

- [38] J. M. Miller, J. Raymond, J. Homan, A. C. Fabian, D. Steeghs, R. Wijnands, M. Rupen, P. Charles, M. van der Klis, and W. H. G. Lewin, *ApJ* **646**, 394 (2006).
- [39] G. Ponti, R. P. Fender, M. C. Begelman, R. J. H. Dunn, J. Neilsen, and M. Coriat, *MNRAS* **422**, L11 (2012).
- [40] P. Laurent and L. Titarchuk, *ApJ* **727**, 34 (2011).
- [41] A. A. Zdziarski, J. E. Grove, J. Poutanen, A. R. Rao, and S. V. Vadawale, *ApJ* **554**, L45 (2001).